JOURNAL OF APPLIED CRYSTALLOGRAPHY

Volume 55 (2022)

Supporting information for article:

Highly effective removal of formaldehyde from aqueous solution using mesoporous ε-MnO2 crystals at room temperature

Xuan Liu, Jialin Wu, Qiang Li, Zhaojun Wu and Jianbin Zhang

Highly effective removal of formaldehyde from aqueous solution at near room temperature using mesoporous ε-MnO_2 crystals

Xuan Liu[1,2], Jialin Wu[1,2], Qiang Li[2], Zhaojun Wu[2], and Jianbin Zhang[1,2]*

1 Hebei Provincial Key Lab of Green Chemical Technology and High Efficient Energy Saving, School of Chemical Engineering and Technology, Hebei University of Technology, Tianjin, 300130, China

2 Inner Mongolia Engineering Research Center for CO_2 Capture and Utilization, Inner Mongolia University of Technology, Hohhot 010051, China

*To whom correspondence should be addressed. E-mail: tadzhang@pku.edu.cn (J. B. Zhang)

Materials：HCl (CAS: 7647-01-0), KI (CAS: 7681-11-0), CH_3COOH (CAS: 64-19-7), soluble starch (CAS: 9005-84-9), C_2H_6O (CAS: 64-17-5) and $Na_2S_2O_3·5H_2O$ (CAS: 7772-98-7) were purchased from Yongsheng Fine Chemical Co., Ltd. (Tianjin, China). KIO_3 (CAS: 7758-05-6) and $C_5H_8O_2$ (CAS: 123-54-6) were purchased from Shanghai Mac Biochemical Technology Co., Ltd. NaOH (CAS: 1310-73-2) and CH_3COONH_4 (CAS: 631-61-8) were purchased from Windship Chemical Reagent Technology Co., Ltd.

***Construction of CO_2SM*:** The strategy for the synthesis of CO_2SM has been reported in our previous work (Sha, et al., 2017) and shown as follows: a gas rate of 250 mL/min CO_2 gas (99.9%) is introduced into a binary system (~50 g) of 1,2-PDA and 1,2-PPD mixture (1: 1 molar ratio of the two) at room temperature and atmosphere pressure, and 3-5% secondary water is added to the whole system in which the aim is to reduce the viscosity of the system so that the mass transfer rate becomes faster. Throughout the process as CO_2 gas is introduced, the system becomes viscous at t = 20 min and gives off a lot of heat, continuing to introduce CO_2 gas after t = 24 h a white viscous solid appears

lasting about 2 h before forming a white solid powder. The solid powder was washed 3 times with ethanol and vacuum dried at 60 °C for 12 h to obtain the CO_2SM, which was demonstrated by serial characterizations to be an alkyl ammonium carbonate (Sha, et al., 2017). The specific formation process is shown in Figure S1 and Scheme S1.

Figure S1
Reaction process of 1,2-PDA + 1,2-PPD with CO_2 at different times.

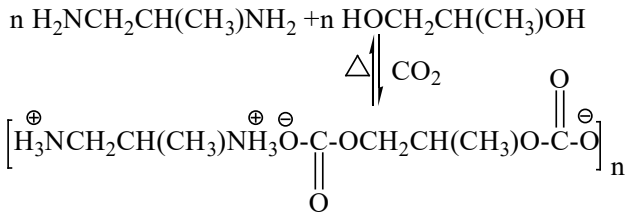

Scheme S1
1,2-PDA + 1,2-PPD and CO_2 reaction equation

***Formaldehyde line drawing*:**

***Preparation of Formaldehyde Standard Reservoirs*:** A 2 mL pipette was used to accurately measure 2.8 mL of (37% formaldehyde) formaldehyde solution in a 1 L volumetric flask to fix the volume. After calibration, a 10 mg/L formaldehyde standard solution was prepared (You, 2018).

***Reservoir fluid calibration*:**Add 1.0 g of KI, 10 mL 0.015 mol/L KIO_3 solution and 10 mL 1 mol/L HCl to six 250 mL iodine measuring flasks labelled 1-6 respectively and leave for 5-10 min. Take 3 of them and add 100 mL boiled cooling water, titrate with 0.05 mol/L $Na_2S_2O_3 \cdot 5H_2O$ solution to light yellow, add 1 mL 0.5% starch solution to the iodine flask, continue titrating until the blue color disappears, the average value of the volume of $Na_2S_2O_3 \cdot 5H_2O$ solution consumed in iodine measuring flasks 1-3 was recorded as V_1; Add 5 mL of the prepared formaldehyde standard reserve solution to

iodine measuring bottles 4-6, add 1.5 mol/L NaOH solution dropwise to light yellow, leave for 10 min, add 15 mL 1 mol/L HCl, leave for 10 min, add 100 mL of boiling cool water, with 0.05 mol/L of $Na_2S_2O_3 \cdot 5H_2O$ solution titrated to light yellow, add 1 mL 0.5% starch solution in iodine measuring flask, continue titration until the blue colour disappears, the average value of the volume of $Na_2S_2O_3 \cdot 5H_2O$ solution consumed in iodine measuring flasks 4-6 was recorded as V_2. Calculate the concentration of the formaldehyde standard stock solution according to the following formula:

$$c=0.015\times3\times10.0\times30（V_1-V_2）/5.0V_1 \quad (1)$$

Formula: c is the concentration of formaldehyde standard stock solution, g/L; 0.015 is the concentration of KIO_3 standard solution, mol/L; 10.0 is the volume of KIO_3 standard solution, mL; 30 is the molar mass of formaldehyde, g/mol; 5.0 is the volume of formaldehyde standard stock solution, mL; V_1, V_2 is the average volume of $Na_2S_2O_3 \cdot 5H_2O$ solution consumed, mL. In this work, the concentration of formaldehyde reservoir was measured according to equation (1) as 0.9619 g/L.

***Standard curve plotting*:** Formulate the standard formaldehyde stock solution according to equation (1) into 10 mg/L of formaldehyde standard use solution. Nine 50 mL volumetric flasks numbered 1-9 were taken, into which volumes of 0, 5, 10, 15, 20, 25, 30, 40 and 50 mL of formaldehyde standard use solution were pipetted and fixed to 50 mL, 2.5 mL of acetylacetone solution was added respectively and then the water bath was thermostated at (60 ± 2)℃ for 15 min, cooled for 1 h, and the absorbance was measured at a wavelength of 413 nm with distilled water as blank control, determine the absorbance of 1-9 and record the data. The standard curve for formaldehyde was plotted, where the horizontal coordinate is the concentration of formaldehyde and the vertical coordinate is the corresponding absorbance. The equation $y = 0.1946x+0.0266$ can be derived from Figure. S2 and the correlation coefficient between the two is 0.9987.

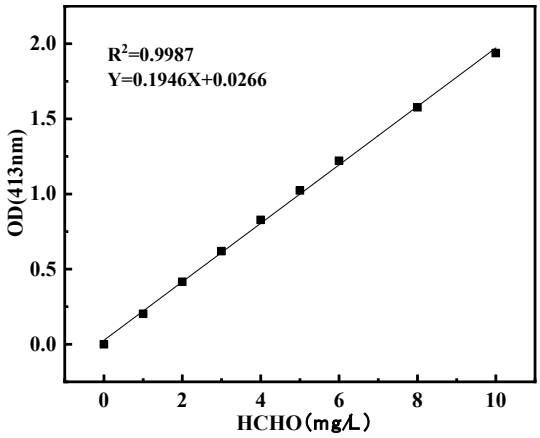

Figure S2
Standard curves for the determination of formaldehyde.

***Formaldehyde determination method*:** Formaldehyde was determined by reference to HJ 601-2001 (Ministry of Environmental Protection, 2011), formaldehyde reacted with acetylacetone solution at about 60 °C in a buffered solution of acetic acid and ammonium acetate at pH = 6 to form a yellow complex, and the colour of this complex was linearly related to the concentration of formaldehyde at a wavelength of 413 nm. The absorbance of the aqueous solution of the complex was therefore determined using a UV spectrophotometer and the formaldehyde concentration was then derived from the standard curve. The procedure is as follows: take an appropriate amount of the sample to be measured in a 25 mL stoppered cuvette, dilute to the scale line with distilled water, add 2.5 mL of acetylacetone solution and shake well, thermostat at (60 ± 2) °C for 15 min, cool for 1 h and then measure the absorbance at a wavelength of 413 nm with distilled water as a blank control. Calculate the concentration of formaldehyde in the sample being measured based on the lines drawn in Figure. S2.

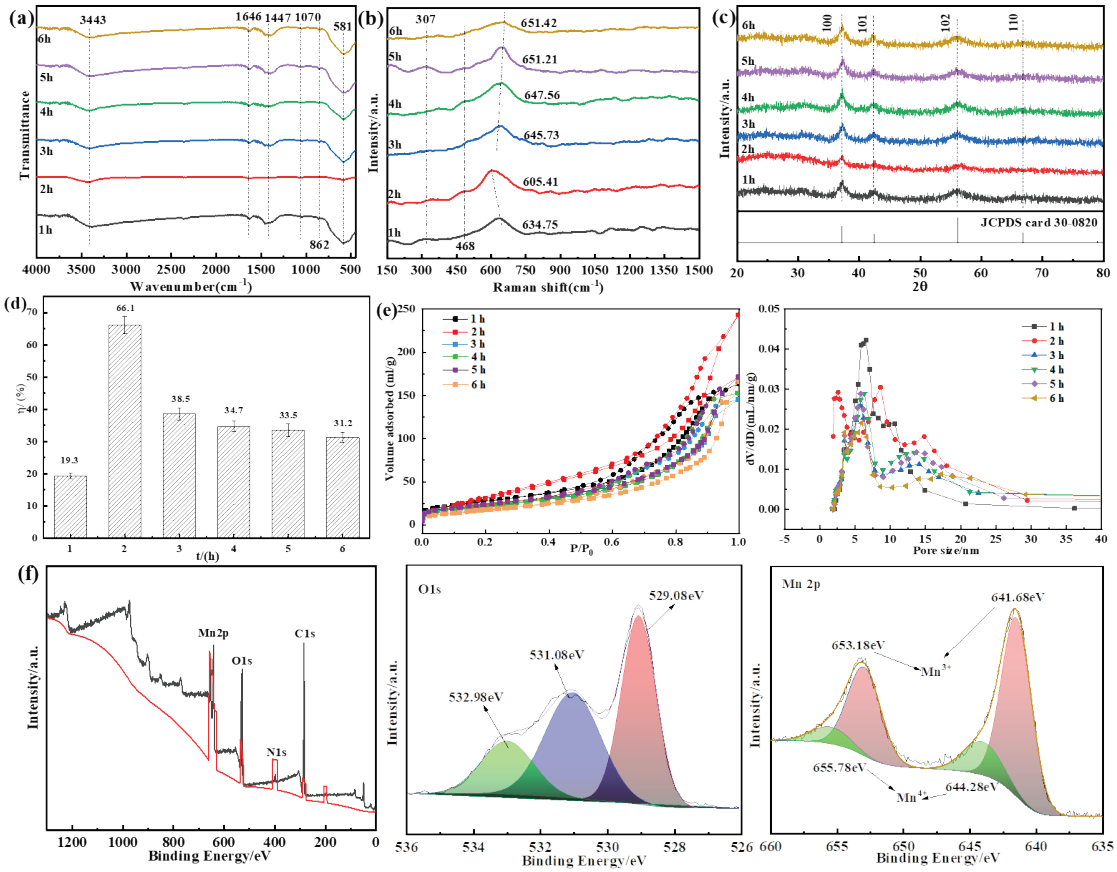

Figure S3

(a) FTIR pattern of the catalyst, (b) Raman pattern of the catalyst, (c) XRD pattern of the catalyst, (d) Degradation rate of catalyst to 10 mL 10 mg/L HCHO solution at 25℃, (e) N_2 adsorption-desorption isotherm and pore size distribution of the catalyst and (f) XPS pattern of the catalyst (t = 2 h).

Table S1

N_2 adsorption-desorption results of ε-MnO_2 prepared at different hydrothermal times.

Catalysts	$S_{BET}/m^2 \cdot g^{-1}$	Pore Volume/mL/g	Pore Size/nm
1h	99.5	0.2518	10.12
2h	134.3	0.3695	11.01
3h	82.5	0.2226	10.80
4h	80.8	0.2344	11.60
5h	86.9	0.2613	12.02
6h	66.5	0.2498	15.02

Table S2

XPS results of ε-MnO_2 prepared at different hydrothermal times.

Catalysts	HCHO degradation rate(%)	O_{ads}/O_{latt}	Mn^{3+}/Mn^{4+}
1h	19.3	1.32	3.82

2h	66.1	1.34	4.21
3h	38.5	0.84	5.66
4h	34.7	0.88	5.42
5h	33.5	1.09	5.82
6h	31.2	0.78	5.40

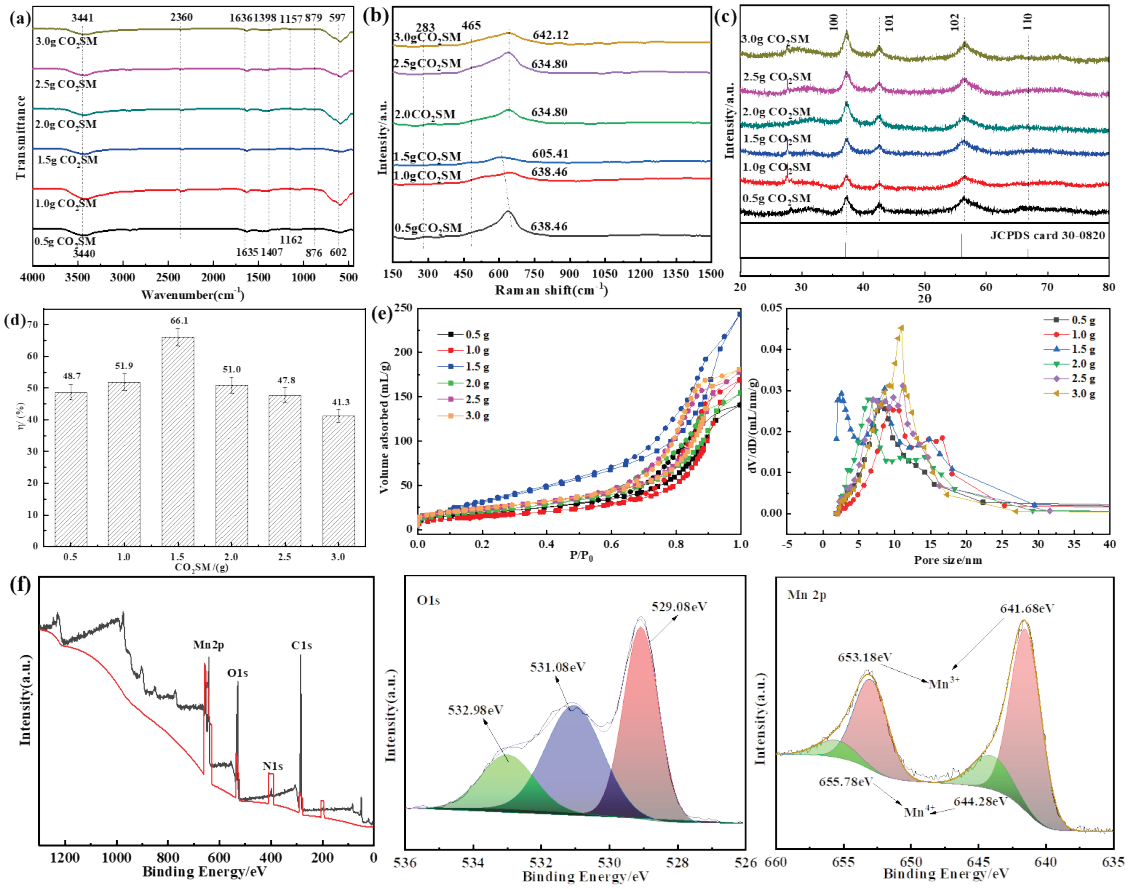

Figure S4

(a) FTIR pattern of the catalyst, (b) Raman pattern of the catalyst, (c) XRD pattern of the catalyst, (d) Degradation rate of catalyst to 10 mL 10 mg/L HCHO solution at 25℃, (e) N_2 adsorption-desorption isotherm and pore size distribution of the catalyst and (f) XPS pattern of the catalyst (CO_2SM = 1.5 g).

Table S3

N_2 adsorption-desorption results of ε-MnO_2 prepared at different CO_2SM dosages.

Catalysts	$S_{BET}/m^2 \cdot g^{-1}$	Pore Volume/mL/g	Pore Size/nm
0.5g	55.1	0.2153	12.49
1.0g	68.9	0.2575	18.52
1.5g	134.3	0.3695	11.01
2.0g	76.3	0.2349	12.31

2.5g	86.3	0.2727	12.63
3.0g	86.9	0.2784	12.81

Table S4

XPS results of ε-MnO_2 prepared at different CO_2SM dosages.

Catalysts	HCHO degradation rate(%)	O_{ads}/O_{latt}	Mn^{3+}/Mn^{4+}
0.5g	48.7	0.90	4.39
1.0g	51.9	1.11	5.11
1.5g	66.1	1.34	4.21
2.0g	51.0	1.09	4.60
2.5g	47.8	1.05	4.78
3.0g	41.3	0.92	5.13

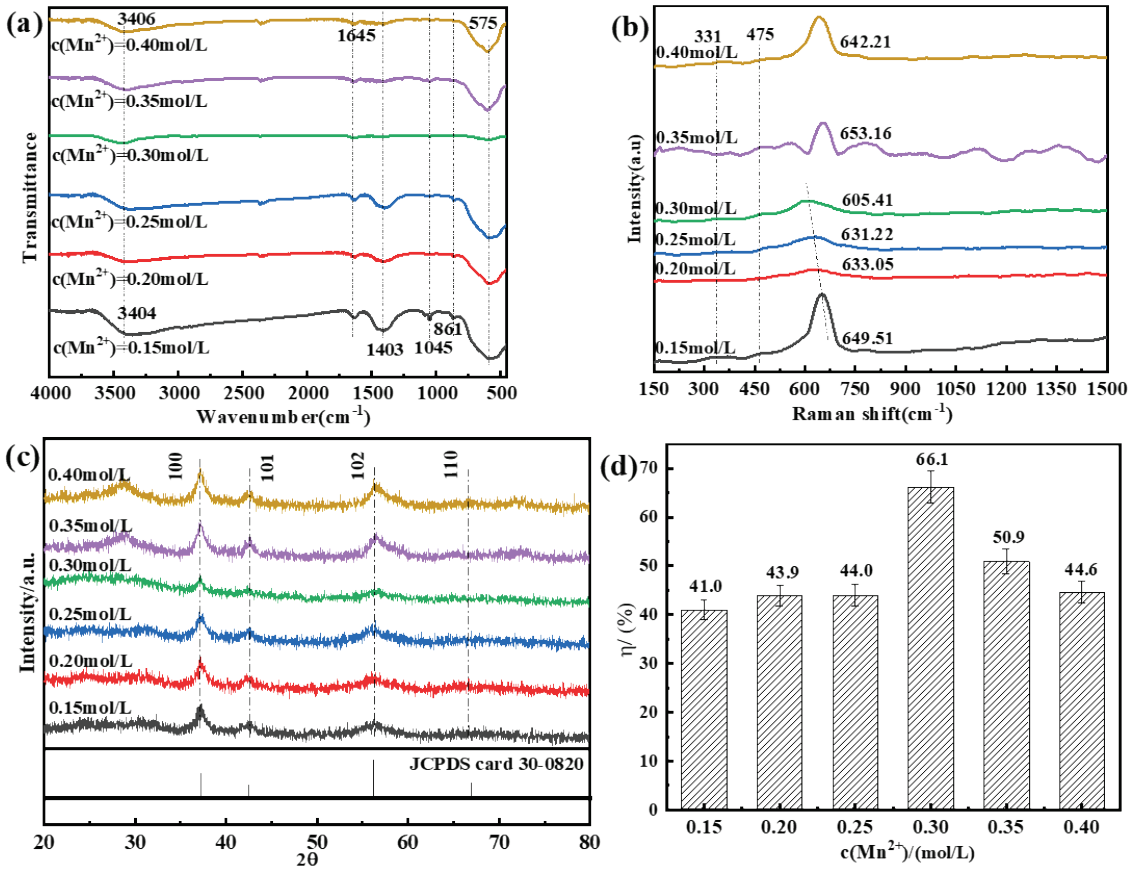

Figure S5

(a) FTIR pattern of the catalyst, (b) Raman pattern of the catalyst, (c) XRD pattern of the catalyst and (d) Degradation rate of catalyst to 10 mL 10 mg/L HCHO solution at 25℃.

***Regression model selection*:** The experimental data were fitted to a linear model, a two-factor model (2FI), a quadratic model and a cubic model. The specific fitted parameters are listed in Table S5 as a means of selecting the appropriate model for this experiment.

Table S5
Results of fitting experimental data to each model.

Source model	Sequential P value	Std. Dev	R-Squared	Adjusted R-Squared	Predicted R-Squared	Df	PRESS	
Linear	0.0049	8.93	0.4505	0.3589	0.2630	20	2566.61	
2FI	0.7620	9.48	0.5359	0.2781	0.0236	14	3400.50	
Quadratic	< 0.0001	4.15	0.9306	0.8613	0.6005	10	1391.43	Suggested
Cubic	0.6897	4.57	0.9641	0.8323	-4.1757	2	18024.96	Aliased

The residuals are important data for judging the accuracy of the model (Feng, et al., 2021). Figure S6(a) shows that all the residuals of the quadratic model are linearly distributed, Figure S6(b) shows that the residuals are loosely and irregularly distributed with the predicted values of the model and Figure S6(c) shows that the predicted values of the quadratic polynomial model are more consistent with the actual values of the data in the whole investigation area. This is good evidence of the correctness and accuracy of the chosen model.

As can be seen from Table S5, the quadratic polynomial model fitted significantly at the 95% confidence level (P-value < 0.0001), and the smaller standard deviation of the quadratic polynomial model (4.15) compared to the other models indicates that it fitted better in the region under investigation. Secondly, the coefficient of determination of the quadratic polynomial model R^2 = 0.9306 indicated that the four factors studied (CO_2SM dosage (g),

reaction temperature (℃), reaction time (h) and c(Mn^{2+}) concentration (mol/L) had 93.06% effect on the degradation of HCHO by ε-MnO_2. And the correction coefficient Adj. R^2 = 0.8613 indicated that after the adjustment of the quadratic polynomial model the four factors had 86.13% effect on the experimental response values, indicating that the four factors were correctly selected and were important factors for the quadratic model. In general, the smaller the coefficient of variation C.V.% the more reliable the model (Feng, et al., 2021), this experiment C.V.%=7.86 %<10 % then the response surface regression model is true and reliable; secondly, the precision Adeq Precision can reflect the signal-to-noise ratio of the experiment is generally better than 4 (Feng, et al., 2021), this experiment precision reaches 12.14 which means the data is reliable.

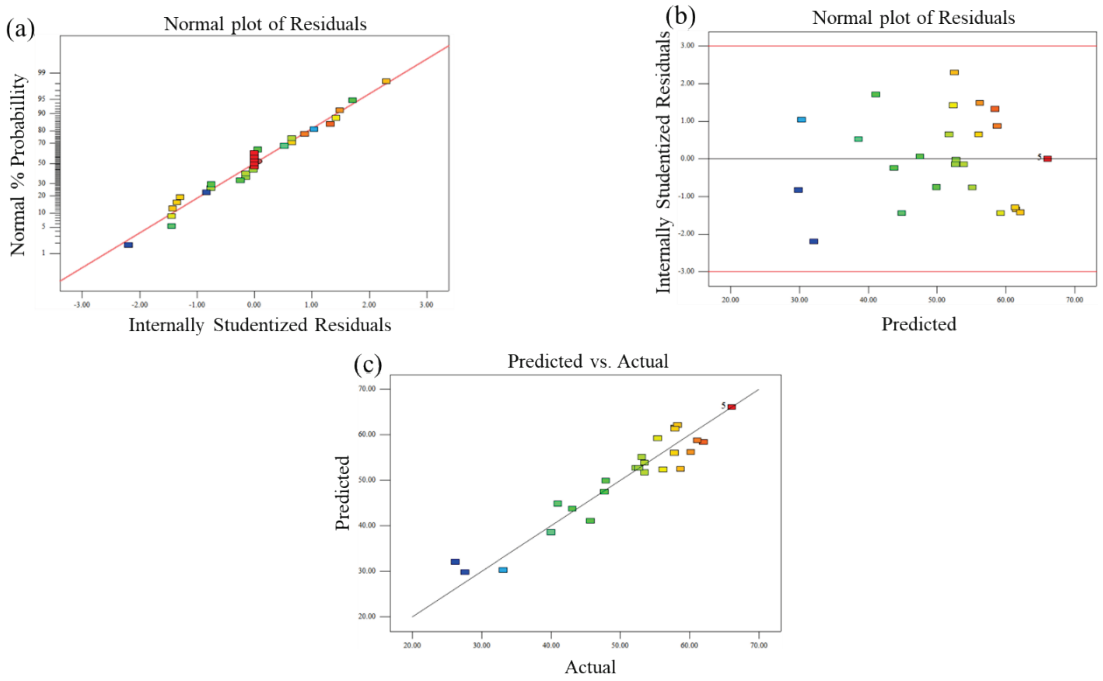

Figure S6

(a) Plot of normal distribution of residual data; (b) Residuals versus equation prediction correspondence diagram; (c) Plot of predicted versus measured values for the quadratic model.

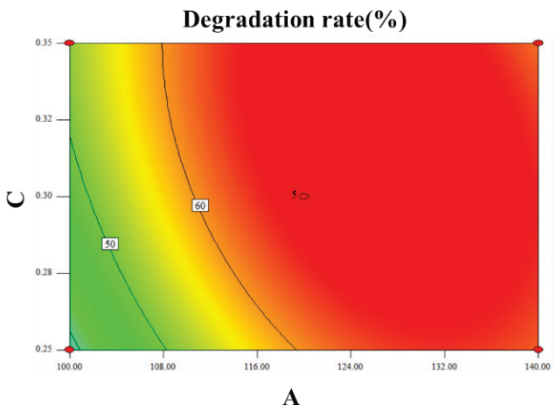
Degradation rate(%)
C
A
50
60
50

(b)

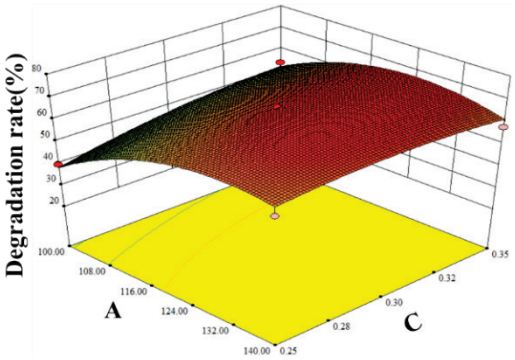
Degradation rate(%)
A
C

(c)

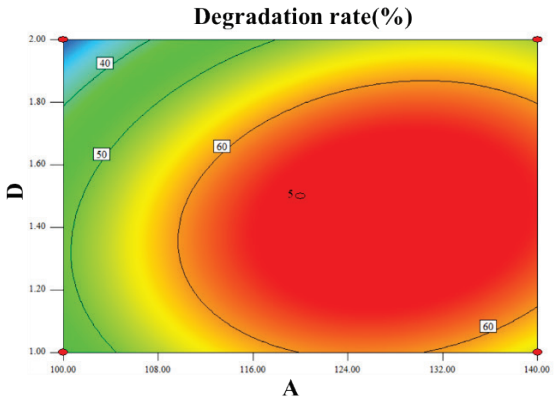
Degradation rate(%)
D
A
40
50
60
50
60

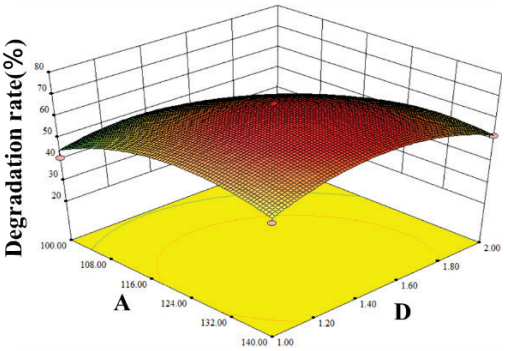
Degradation rate(%)
A
D

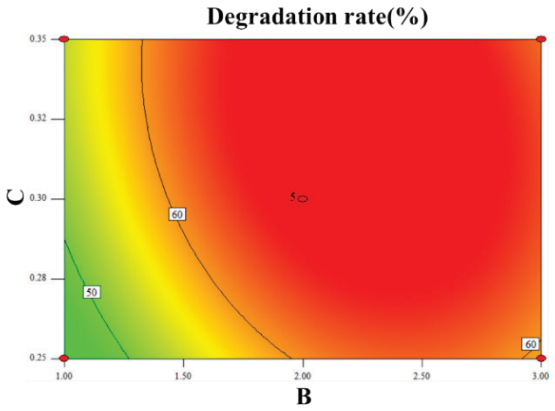
Degradation rate(%)
C
B
50
60
50
60

(d)

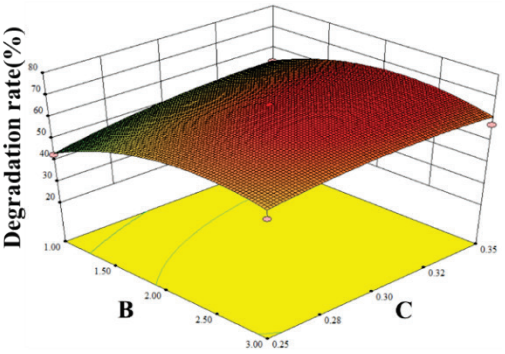
Degradation rate(%)
B
C

(e)

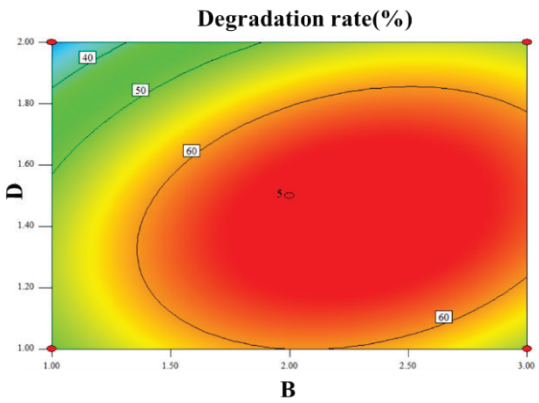
Degradation rate(%)
D
B
40
50
60
50
60

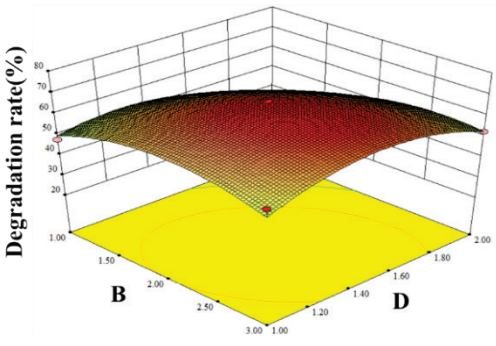
Degradation rate(%)
B
D

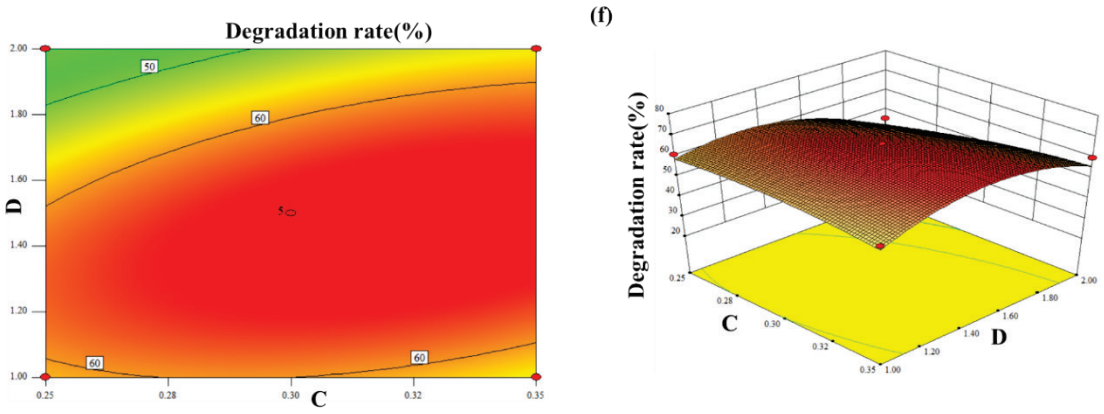

Figure S7

Response surface and contour plots of the effect of the interaction of ((b) A and C, (c) A and D, (d) B and C, (e) B and D, (f) C and D) on the degradation of HCHO by ε-MnO_2.

***Response surface analysis*:** From Figure S7(b), it can be seen that when the reaction temperature T(℃) is small, the HCHO degradation rate increases and then decreases with the increase of $c(Mn^{2+})$; when $c(Mn^{2+})$ is small, the HCHO degradation rate increases and then decreases with the increase of the reaction temperature T(℃), and at the reaction temperature T(℃) = 120 ℃ and $c(Mn^{2+})$ = 0.3 mol/L there is a extremely large value point with 66.1% HCHO degradation. From Figure S7(c), it can be seen that when the reaction temperature T(℃) is small, the HCHO degradation rate increases and then decreases with the increase of $CO_2SM(g)$ dosage; when the dosage of $CO_2SM(g)$ is small, the HCHO degradation rate increases and then decreases with the increase of the reaction temperature T(℃), and at the reaction temperature T(℃) = 120 ℃ and $CO_2SM(g)$ dosage = 1.5 g the response surface plot There was a great value point with HCHO degradation rate of 66.1%. From Figure S7(d), it can be seen that the HCHO degradation rate increased and then decreased with the increase of $c(Mn^{2+})$ when the reaction time t(h) was small, and increased and then decreased with the increase of the reaction time t(h) when $c(Mn^{2+})$ was small, and there was a great value point in the response surface plot at the reaction time t(h) = 2 h and $c(Mn^{2+})$ = 0.3 mol/L, and the HCHO degradation rate was 66.1%. From Figure S7(e), it can be seen that when the reaction time t(h) is small, the HCHO degradation rate increases and then decreases with the increase of $CO_2SM(g)$ dosage; when the

$CO_2SM(g)$ dosage is small, the HCHO degradation rate increases and then decreases with the increase of reaction time t(h), and at the reaction time t(h)=2 h and $CO_2SM(g)$ dosage = 1.5 g the response surface plot has an extreme value point, the HCHO degradation rate was 66.1%. From Figure S7(f), it can be seen that the HCHO degradation rate increased and then decreased with the increase of $CO_2SM(g)$ when $c(Mn^{2+})$ was small, the HCHO degradation rate increased and then decreased with the increase of $c(Mn^{2+})$ when $CO_2SM(g)$ was small, and the response surface plot at $c(Mn^{2+})$ = 0.3 mol/L and $CO_2SM(g)$ = 1.5 g There was an extreme value point in the response surface plot with 66.1% HCHO degradation rate.

***Optimization of reaction conditions*:**

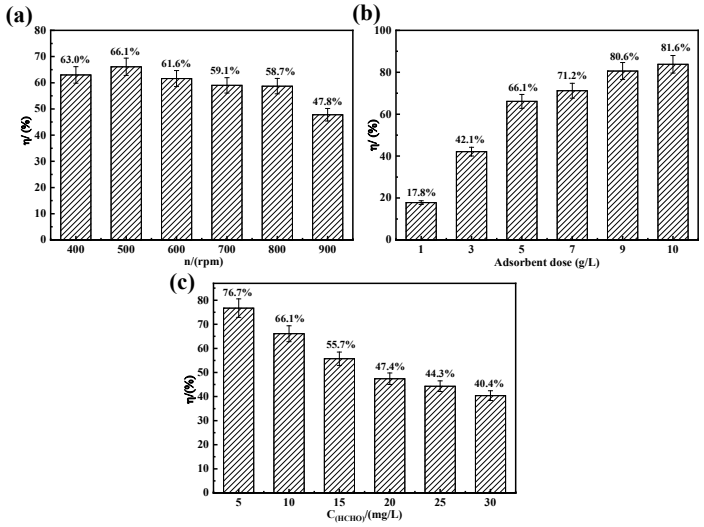

Figure S8

Rotational speed effects (a), Different dosing rates (b) and HCHO solutions of different concentrations (c) on the degradation of HCHO.

At a reaction temperature of 25 °C, an HCHO concentration of 10 mg/L and an ε-MnO_2 dosage of 5 g/L, it can be seen from Figure S8(a) that the rotational speed had a significant effect on the degradation rate of HCHO. This was due to the fact that the violent vibration increased the collision between HCHO molecules and ε-MnO_2 catalyst, which provided more opportunities for the binding of HCHO molecules to the adsorption sites on the ε-MnO_2 catalyst (Gupta, et al., 2015). However, the removal rate of HCHO decreased as the rotational speed continued to increase. This was due to

the fact that too large a rotational speed made the binding of HCHO molecules to the sample less stable, so the rotational speed n = 500 rpm was chosen as the optimal speed for subsequent experiments. At a reaction temperature of 25 °C, an HCHO concentration of 10 mg/L and a rotational speed of 500 rpm, the effects of ε-MnO_2 catalysts at 1 g/L, 3 g/L, 5 g/L, 7 g/L, 9 g/L and 10 g/L on the degradation rate of HCHO were investigated respectively. It can be seen from Figure S8(b) that with the increase of catalyst dosage, the degradation rate of HCHO showed an increasing trend, and at the catalyst dosage of 5 g/L, the degradation rate of HCHO was 66.1%, the HCHO degradation rate gradually plateaued and increased insignificantly when the dosage was over 5 g/L.This is because a dynamic equilibrium was reached between the ε-MnO_2 catalyst and the HCHO solution (Giraldo, et al., 2014). In order to optimize the HCHO degradation rate and avoid wasting resources, 5 g/L ε-MnO_2 catalyst was selected for the subsequent experiments. The effect of ε-MnO_2 catalyst on the degradation rate of different concentrations of HCHO solutions was investigated under the reaction conditions of 25 ℃, 5 g/L dosage and 500rpm. From Figure S8(c), it is obvious that the ε-MnO_2 catalyst showed good degradation rates for different concentrations of HCHO solutions, and the degradation rates for low concentrations of 5 mg/L and 10 mg/L HCHO solutions could reach over 65%.

Table S6

Parameters associated with Langmuir and Freundlich adsorption isotherms and R^2.

Temperature (K)	Langmuir			Freundlich		
298.15	q_{max}(mg·g^{-1})	K_L(L·mg^{-1})	R^2	K_F	n	R^2
	2..46	0.3048	0.9817	0.7323	2.5680	0.9771

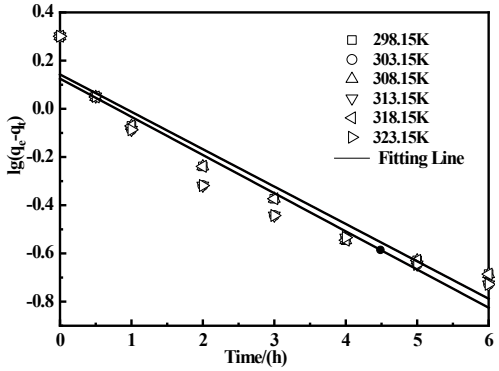

Figure S9

Kinetic fits at different temperatures (quasi-first-order fit).

Table S7

Quasi first order kinetic fit R^2 at different temperatures.

T(K)	298.15	303.15	308.15	313.15	318.15	323.15
R^2	0.9301	0.9114	0.9301	0.9114	0.9301	0.9114

Table S8

Quasi-secondary kinetic fit R^2 at different temperatures.

T(K)	298.15	303.15	308.15	313.15	318.15	323.15
R^2	0.9988	0.9998	0.9999	0.9991	0.9997	0.9966

Table S9

Thermodynamic fit at different temperatures.

T/(K)	ΔG^0(kJ/mol)	ΔH^0(kJ/mol)	ΔS^0(J/mol·K)
298.15	-26.713	65.546	309.211
303.15	-27.830		
308.15	-30.490		
313.15	-30.760		
318.15	-32.780		
323.15	-34.495		

References

[1] Sha, F., Guo, B., Zhao, J., Zhang, F., Qiao, X., Ma, L., liu, C., Zhang, J. (2017). Green. Energy. Environ. **2**, 401-411.

[2] You, T. (2008). Chemical. Reagents. **30(6)**, 2, 447-448.

[3] Ministry of Environmental Protection (2011). Qinghai Environmental Protection. Water Quality Determination of Formaldehyde Acetylacetone Spectrophotometric Method.

[4] Feng, Q., Chen, X., Peng, Z., Zheng, Y. (2021). Colloid. Surface. A. **627**, 127-177.

[5] Gupta, A., Balomajumder, C. (2015). J. Environ. Chem. Eng. **3(2)**, 785-796.

[6] Giraldo, L., Moreno-Piraján, J. C. (2014). J. Anal. Appl. Pyrol. **106**, 41-47.